

# Quantum size effect on the dissociation of O<sub>2</sub> molecules on ultrathin Pb(111) films

Ziyu Hu,<sup>1,2</sup> Yu Yang,<sup>2</sup> Bo Sun,<sup>2</sup> Xiaohong Shao,<sup>1</sup> Wenchuan

Wang,<sup>3</sup> Xucun Ma,<sup>4</sup> Qikun Xue,<sup>5</sup> and Ping Zhang<sup>2,\*</sup>

<sup>1</sup>*College of Science, Beijing University of Chemical Technology,  
Beijing 100029, People's Republic of China*

<sup>2</sup>*LCP, Institute of Applied Physics and Computational Mathematics,  
P.O. Box 8009, Beijing 100088, People's Republic of China*

<sup>3</sup>*Laboratory of Molecular and Materials Simulation,  
Key Laboratory for Nanomaterials of Ministry of Education,  
Beijing University of Chemical Technology,  
Beijing 100029, People's Republic of China*

<sup>4</sup>*Institute of Physics, Chinese Academy of Sciences,  
Beijing 100080, People's Republic of China*

<sup>5</sup>*Department of Physics, Tsinghua University,  
Beijing 100084, People's Republic of China*

## Abstract

Using first-principles calculations, we systematically study the dissociation of O<sub>2</sub> molecules on different ultrathin Pb(111) films. Based on our previous work revealing the molecular adsorption precursor states for O<sub>2</sub>, we further explore that why there are two nearly degenerate adsorption states on Pb(111) ultrathin films, but no precursor adsorption states exist at all on the Mg(0001) and Al(111) surfaces. And the reason is concluded to be the different surface electronic structures. For the O<sub>2</sub> dissociation, we consider both the reaction channels from gas-like and molecularly adsorbed O<sub>2</sub> molecules. We find that the energy barrier for O<sub>2</sub> dissociation from the molecular adsorption precursor states is always smaller than from O<sub>2</sub> gases. The most energetically favorable dissociation process is found to be the same on different Pb(111) films, and the energy barriers are found to be modulated by the quantum size effects of Pb(111) films.

## I. INTRODUCTION

The adsorption and dissociation of  $O_2$  molecules on metal surfaces are of great importance to the subsequent oxidation reactions and to the formation of metal oxides<sup>1</sup>. This is especially true for the formation of thin oxide films that have been widely used as catalysts, sensors, dielectrics, and corrosion inhibitors<sup>2</sup>. Thus vast studies have been carried out on the  $O_2$  adsorption and dissociation on metal surfaces. During these studies, the theoretical *ab initio* modeling based on the adiabatic approximation has been proved successful over a wide range for studying the adsorption and dissociation of  $O_2$  on transition metal surfaces. By calculating the adiabatic potential energy surface (PES), it has been found that  $O_2$  molecules will spontaneously dissociate while adsorbing at reactive transition metal surfaces like iron (Fe)<sup>3</sup>. For noble transition metals like gold (Au)<sup>4</sup>, silver (Ag)<sup>5</sup>, Copper (Cu)<sup>6</sup>, platinum (Pt)<sup>4,7</sup> and Nickel (Ni)<sup>7</sup>, the adsorption of  $O_2$  turns out to depend on the ambient temperature, and both atomic and molecular adsorptions have been observed. Remarkably, in all above transition metal systems, the concept of adiabatic calculation works very well in explaining and predicting a large amount of physical/chemical phenomena during dissociation process of  $O_2$ . When the attention is focused on the nontransition metals with only *sp* valence electrons, an uncomfortable gap opens between *ab initio* prediction and experimental observation. The most notable is the long-term enigma of low initial sticking probability of thermal  $O_2$  molecules at Al(111), which has been measured by many independent experiments<sup>8,9</sup> but cannot be reproduced by adiabatic state-of-the-art density functional theory (DFT) calculations<sup>10-12</sup>. The central problem is that the adiabatic DFT calculations were unable to find any sizeable barriers on the adiabatic PES, which has led to speculations that nonadiabatic effects may play an important role in the oxygen dissociation process at the Al(111) surface<sup>11,13-18</sup>. Recently, we present a comparative study on the electronic structure of an  $O_2$  molecule in close to the Be(0001), Mg(0001) and Al(111) surfaces, and find that the triplet state of  $O_2$  is influenced by the Mg(0001) and Al(111) surfaces, but not by the Be(0001) surface<sup>19</sup>. Thus we prove that the adiabatic DFT calculations are still reliable to study the  $O_2$ /Be(0001) system, and find out sizable dissociation energy barriers for  $O_2$  molecules on the Be(0001) surface<sup>19</sup>. However, in contrast to the systematical results on the  $O_2$  dissociation on transition metal surfaces, there are still no criteria to judge whether an energy barrier is needed or whether a precursor molecular-adsorption state exists

for the  $O_2$  dissociation on *sp* metal surfaces. Motivated by these backgrounds, in this paper we investigate the dissociation of  $O_2$  molecules on another *sp* metal surface, lead (Pb). We find that the adiabatic DFT calculation also leads to reliable results for the  $O_2$ /Pb(111) system.

Another motive for us to study the  $O_2$  dissociation on the Pb(111) surface is that atomically uniform Pb films with thickness from several to tens of monolayers (MLs) have been successfully fabricated on both metal and semiconductor substrates<sup>20,21</sup>, which can serve as an ideal prototype for experimental researchers to investigate the surface oxidation of Pb. However, it is believed that for very thin metal films, the adsorption and dissociation of  $O_2$  molecules becomes more complex because of the two boundaries. According to the “particle-in-a-box” model, electrons confined in a uniform film are quantized into discrete energy levels along the film-normal direction, forming the so-called quantum well states. Because the electron Fermi wavelength of Pb is nearly 4 times the lattice spacing along the [111] direction<sup>22</sup>, many properties like thermal stability, surface energy, and work function of the Pb films oscillate with thickness with a quasibilayer period<sup>23–25</sup>. Recently, a unique two-step method has been brought out to efficiently oxidize the the Pb(111) surface<sup>26,27</sup>. During this special oxidation process,  $O_2$  molecules are firstly introduced at a low temperature and adsorb in a precursor state, then the Pb(111) surface is oxidized by a subsequently annealing to room temperature<sup>27</sup>. Most interestingly, both the oxygen coverage at low temperature and oxide coverage after annealing are found to be modulated by the quantum size effect (QSE) of ultrathin Pb(111) films<sup>26</sup>. These studies together with other investigations<sup>28</sup> clearly prove the modulation of surface oxidation by QSE. To understand the complicated experimental observations, the systematical investigations on the adsorption and dissociation of  $O_2$  molecules on ultrathin Pb(111) films are needed.

In our previous work, we have already studied the adsorption properties for both molecular  $O_2$  and atomic O on different Pb(111) films<sup>29,30</sup>. It is found that  $O_2$  molecules will not spontaneously dissociate on Pb(111) films, and a precursor molecular adsorption state exists<sup>29</sup>. Here in this work, we further analyze the electronic interactions for the adsorption of  $O_2$ , investigate the dissociation process for  $O_2$ , and study the QSE on the dissociation energy barriers. The rest of the paper organized as follows. In Sec. II, we give details of the first-principles total energy calculations, which is followed in Sec. III by our analysis for the adsorption state of  $O_2$  on the Pb(111) surface. In Sec. IV, we study the  $O_2$  dissociation

on Pb(111) films, and discuss the QSE on the corresponding energy barriers. And finally in Sec. VI, we give our conclusions.

## II. COMPUTATIONAL METHODS

The DFT total energy calculations are carried out using the Vienna *ab initio* simulation package<sup>31</sup>. The generalized gradient approximation (GGA) of Perdew *et al.*<sup>32</sup> and the projector-augmented-wave (PAW) potentials<sup>33</sup> are employed to describe the exchange-correlation energy and the electron-ion interaction, respectively. The so-called “repeated slab” geometries<sup>34</sup> are employed to model the clean Pb(111) films ranging from 4 to 8 monolayers (ML). A vacuum layer of 20 Å is adopted to separate the Pb(111) slabs in two adjacent cells, which is found to be sufficiently convergent from our test calculations. The O<sub>2</sub> was placed on one side of the slab, namely on the top surface, whereas the bottom layer was fixed. All other Pb layers as well as the oxygen atoms are free to relax until the forces on them are less than 0.02 eV/Å. The plane-wave energy cutoff is set to 400 eV. A Fermi broadening<sup>35</sup> of 0.1 eV is chosen to smear the occupation of the bands around E<sub>F</sub> by a finite-*T* Fermi function and extrapolating to *T*=0 K. Integration over the Brillouin zone is done using the Monkhorst-Pack scheme<sup>36</sup> with 13 × 13 × 1 grid points. The calculated lattice constant of bulk Pb is 5.03 Å, in good agreement with the experimental value of 4.95 Å<sup>37</sup>. The binding energy of spin-polarized O<sub>2</sub> is calculated to be *D*=5.78 eV per atom and the O-O bond length is about 1.235 Å. These results are typical for well-converged DFT-GGA calculations. Compared to the experimental<sup>38</sup> values of 5.12 eV and 1.21 Å for O binding energy and bonding length, the usual DFT-GGA result always introduces an overestimation, which reflects the theoretical deficiency for describing the local orbitals of the oxygen. We will consider this overbinding of O<sub>2</sub> when drawing any conclusion that may be affected by its explicit value.

## III. THE ADSORPTION PROPERTIES OF O<sub>2</sub> ON THE PB(111) SURFACE

The geometries of ultrathin Pb(111) films are firstly relaxed before our study for the adsorption and dissociation of O<sub>2</sub> molecules. It is found that the surface relaxations display well-defined QSE<sup>29</sup>. Generally speaking, atoms at the outmost layer tend to relax inward.

In contrast, atoms at the second layer tend to relax outward. And both the contraction for the first interlayer and the expansion for the second interlayer exhibit oscillations of bilayer period, reflecting the effect of the quantum well states<sup>25</sup>.

We then check the reliability of our adiabatic calculations. The main reason for the wrong conclusions lead by adiabatic first-principles calculations on the adsorption of O<sub>2</sub> on *sp*-metals lies in that the lowest unoccupied molecular orbital (LUMO) state of O<sub>2</sub> is always aligned with the Fermi level at any distance between the molecule and metal surfaces such as Al(111), allowing a partial filling of the empty molecular orbital<sup>39</sup>. Due to this unphysical (metal-molecule or intramolecule) charge transfer, the adsorption of O<sub>2</sub> on the Al(111) surface is calculated to be dissociative without any energy barriers, which contradicts with the experimental observations of low initial sticking probability at low temperatures<sup>8,9</sup>. In our previous work<sup>19</sup>, we have shown that the unphysical partial filling of the LUMO does not happen during the adsorption of O<sub>2</sub> on the Be(0001) surface, and thus we obtained sizeable energy barriers for the dissociation of O<sub>2</sub>. Here for the O<sub>2</sub>/Pb(111) system, molecular adsorption precursor states exist, so we can not judge the reliability of our calculations by whether a sizable energy barrier exists or not. We calculate and show in Fig. 1(a) the electronic density of states (DOS) of an O<sub>2</sub> molecule in close to a 5 ML Pb(111) film. In comparison with the DOS of O<sub>2</sub> in close to the Mg(0001) and Al(111) surfaces depicted in Figs. 1(b) and (c), we find that the triplet ground state of the O<sub>2</sub> molecule is not influenced at all in close to the Pb(111) film, but totally disturbed by the Mg(0001) and Al(111) surfaces due to the unphysical charge transfers. Therefore, we are sure that the adiabatic DFT calculations will not lead to unphysical conclusions for the O<sub>2</sub>/Pb(111) system, as well as for the O<sub>2</sub>/Be(0001) system.

To facilitate our discussions, we give some notations at first. Formally, there are four high-symmetry sites on the Pb(111) surface, respectively the top (T), bridge (B), hcp (HH), and fcc (FH) hollow sites. Our previous study has already shown that the high-symmetry sites play crucial roles in the adsorption O<sub>2</sub> molecules on Pb(111) films<sup>29</sup>. Therefore we do not consider other surface sites any more. At each surface site, an O<sub>2</sub> molecule has three different high-symmetry orientations, respectively along the x (i.e.,  $[0\bar{1}1]$ ), y (i.e.,  $[\bar{2}11]$ ), and z (i.e.,  $[111]$ ) directions. Therefore, we will use T-*x, y, z*, B-*x, y, z*, HH-*x, y, z*, and FH-*x, y, z* to respectively represent the 12 high symmetry adsorption channels for O<sub>2</sub>.

After geometry optimizations by initially setting the O<sub>2</sub> molecule at 4.0 Å along each

adsorption channel, we have got 6 molecular adsorption states for  $O_2$ <sup>29</sup>. By using numbers 1, 2, and 3 to represent the  $O_2$  orientation along the x, y, and z directions, we name the six adsorption states respectively as HH1, HH2, HH3, FH1, FH2, and FH3. The atomic geometries for the HH1, HH2 and HH3 states are listed in Figs. 2(b), (c) and (d) respectively. The geometries for the FH1, FH2 and FH3 states are very similar to HH1, HH2 and HH3 states, with the adsorbed oxygen atoms at fcc hollow sites instead of hcp hollow sites. Among the six precursor states, HH1 and HH2 are the most stable and two nearly degenerate states. In our previous work, we have already discussed in detail the interactions between oxygen and Pb for the HH1 state<sup>29</sup>. Here we further analyze the electronic interactions for the HH2 state to discuss why the two adsorption states with different  $O_2$  orientations (i.e. HH1 and HH2 states) are almost degenerate.

Figure 3 shows the calculated difference charge density  $\Delta\rho(\mathbf{r})$  for the HH2 state on the 5 ML Pb(111) film, which is obtained by subtracting the electron densities of noninteracting component systems,  $\rho^{Pb(111)}(\mathbf{r}) + \rho^{O_2}(\mathbf{r})$ , from the density  $\rho(\mathbf{r})$  of the HH2 state, while retaining the atomic positions of the component systems at the same location as in HH2. A positive  $\Delta\rho(\mathbf{r})$  here represents charge accumulation, whereas a negative  $\Delta\rho(\mathbf{r})$  represents charge depletion. Figure 3(a) clearly shows a charge transfer from Pb to  $O_2$ , which is consistent with the electronegativity difference between O and Pb atoms, and same with what we found for the HH1 state<sup>29</sup>. The contour plot for  $\Delta\rho(\mathbf{r})$  in the plane containing the two O atoms and parallel to the Pb surface is shown Fig. 3(b), we can see that there is an electron depletion area in the middle of the two oxygen atoms, indicating the donation of electrons from bonding orbitals of  $O_2$  to Pb. We can also see two electron accumulation areas around the two oxygen atoms indicating the back donation of electrons from Pb to the  $\pi_p^*$  antibonding orbital of  $O_2$ . This interaction mechanism of  $O_2$ -to-surface donation and surface-to- $O_2$   $\pi_p^*$  back donation is just the same with that in the HH1 state<sup>29</sup>. So it is no wonder that the two adsorption states are nearly degenerate and have similar adsorption energies.

In comparison with the Be(0001), Mg(0001) and Al(111) surfaces, Pb(111) is unique in that a parallel  $O_2$  molecularly adsorbs only on it. This is because of the different surface electronic structures. As shown in Fig. 4, the  $p$  electronic states around the Fermi energy strongly hybridize with  $s$  states for both the Mg and Al surfaces (also for the Be(0001) surface<sup>19</sup>), but does not hybridize at all for the Pb(111) surface. As we have seen<sup>29</sup>, the

interaction between O<sub>2</sub> and the Pb(111) surface is mainly contributed by the electronic hybridizations between the frontier molecular orbitals (the orbitals nearest to the Fermi energy) of O<sub>2</sub> and electronic states of Pb. According to the frontier orbital theory, the interactions between O<sub>2</sub> and other metals have similar mechanisms. However, the frontier orbitals of O<sub>2</sub> (i.e.  $\sigma_p$ ,  $\pi_p$ , and  $\pi_p^*$ ) are composed of  $p$  electrons of oxygen, thus they are more compatible with  $p$  electronic states than  $sp$  hybridized electronic states. This compatibility between frontier orbitals of O<sub>2</sub> and  $p$  states of Pb finally leads to the molecular adsorption precursor states.

#### IV. DISSOCIATION OF O<sub>2</sub> MOLECULES

After the studies and discussions for the adsorption on different Pb(111) films, we now investigate the O<sub>2</sub> dissociation. Because of the existence of precursor states, there are two different kinds of dissociation processes for O<sub>2</sub>, respectively from O<sub>2</sub> gases and from the molecular adsorption states. Because the adiabatic calculations have been proved reliable for the O<sub>2</sub>/Pb(111) system, we will calculate the adiabatic one-dimensional (1D) and two-dimensional (2D) potential energy surface (PES) cuts to evaluate the dissociation energy barriers for O<sub>2</sub> molecules.

The 1D PES cuts for an O<sub>2</sub> molecule along the T- $x, y$  and B- $x, y$  channels are show in Fig. 5, together with the O-O bond length as functions of the O<sub>2</sub> height  $h$  from the 5 ML Pb(111) film surface. The adsorption from O<sub>2</sub> gas along the FH- and HH- $x, y$  channels will evolve into the molecular adsorption precursor states. Clearly, the dissociative adsorption of O<sub>2</sub> along the T- $x, y$  and B- $y$  channels are direct and activated, but no dissociative adsorption is found for an O<sub>2</sub> molecules along the B- $x$  channel. This is different from the O<sub>2</sub>/Be(0001) system, where the O<sub>2</sub> dissociation along B- $x$  channel also occurs<sup>19</sup>. Among the calculated channels, the lowest dissociation energy barrier is found to be 0.36 eV along the B- $y$  channel, with the O-O bond length and O<sub>2</sub> height at the transition state to be 1.33 and 2.20Å. The 1D PES cuts along the T- $x, y$  channels have similar distributions, and the corresponding energy barriers are 0.68 and 0.59 eV.

The electronic interactions are then analyzed for the dissociation process from O<sub>2</sub> gases. Figure 6 shows the PDOS for an O<sub>2</sub> molecule at the initial, transition and final states of the dissociation path along the B- $y$  channel. We can see that at the initial state, the O<sub>2</sub>

molecule keeps its triplet electronic structure. As we have discussed, the LUMO of  $O_2$  is above the Fermi energy, proving the reliability of our adiabatic DFT calculations. The highest occupied molecular orbital (HOMO) and LUMO are the spin-up and spin-down antibonding  $\pi_p^*$  molecular orbitals, respectively. Besides of HOMO and LUMO,  $p$  electrons of  $O_2$  make up of two bonding orbitals,  $\sigma_p$  and  $\pi_p$ . For both spins, the  $\sigma_p$  orbitals are lower in energy than the  $\pi_p$  orbitals. When the  $O_2$  molecule evolves into the transition state, electrons transfer from the  $\sigma_p$  and  $\pi_p$  molecular orbitals to Pb through hybridizations. As shown in Fig. 6(b), the  $\sigma_p$  and  $\pi_p$  peaks are diminished. We can also see from Fig. 6(b) that the HOMO and LUMO of  $O_2$  are broadened through hybridizations with electronic states of Pb. During the electronic hybridizations, the spin splittings for all the  $O_2$  molecular orbitals are all decreased. In the final dissociated adsorption state, the total spin of the adsorption system becomes zero. We can see from Fig. 6(c) that the molecular orbitals of  $O_2$  no longer exist after electronic hybridizations. As discussed in our previous work<sup>30</sup>, the interactions between O and Pb atoms display a mixed ionic/covalent character.

The dissociation of  $O_2$  from the molecular adsorption precursor states are more complicated than from  $O_2$  gases because the formation and breaking of O-Pb bonds during the dissociation of  $O_2$  also need to be considered. Detailed information on the atomic adsorption of oxygen on the Pb(111) surface can help us to simplify the problem. In our previous study<sup>30</sup>, we have found that the O atoms choose to adsorb at hollow sites on the Pb(111) surface. Thus we only need to consider the dissociation of an adsorbed  $O_2$  molecule into different hollow sites. For an  $O_2$  molecule in the HH1 or HH2 state, there are two different dissociation paths, respectively to the atomic adsorption of oxygen at two neighboring fcc and hcp hollow sites and to the atomic adsorption of oxygen at two fcc hollow sites. The calculated 2D PES cuts for the adsorbed  $O_2$  molecules in HH1 and HH2 states to dissociate into two neighboring hollow sites are shown in Figs. 7(a) and (b), while the calculated 2D PES cuts for  $O_2$  to dissociate into two fcc hollow sites are also shown in Figs. 7(c) and (d). The calculated energy barriers for these four paths are respectively 0.22, 0.26, 0.59 and 0.37 eV. These values indicate that the most energetically favorable dissociation path for an adsorbed  $O_2$  molecule is from the HH1 adsorption state into the atomic adsorption of oxygen at two neighboring fcc and hcp hollow sites. The saddle point in Fig. 7(a) corresponds to the adsorption structure of two oxygen atoms near two neighboring bridge sites, with their horizontal distance to be 1.40 Å. The smallest energy barriers for an  $O_2$  molecule in the



FH1 and FH2 states to dissociate are both found to be 0.25 eV, which are larger than the smallest energy barrier from the HH1 state of 0.22 eV.

The electronic properties are then analyzed for the dissociation path shown in Fig. 7(a), whose energy barrier is the smallest during the dissociation from molecular adsorption precursor states. The PDOS around the two oxygen atoms are calculated for the corresponding initial, transition and final states. As shown in Fig. 8(a), the  $\pi_p^*$  antibonding orbital of O<sub>2</sub> are broadened and shifted below the Fermi energy in the HH1 adsorption state, through hybridizations with  $p$  electronic states of Pb. At the transition state of the dissociation process, the energy interval between the  $\sigma_s$  and  $\sigma_s^*$  orbitals is decreased from 6.58 to 6.24 eV, and the oxygen  $2p$  states hybridize in a different way with electronic states of Pb from that in the HH1 adsorption state. At the end of the dissociation process, the two oxygen atoms relax into two neighboring hollow sites, and the molecular orbitals of O<sub>2</sub> all disappear after electronic hybridizations.

After the systematic studies on the O<sub>2</sub> dissociation in different ways, we reveal that the most energetically favorable one is from the HH1 adsorption state into two neighboring hollow sites. It is always believed that because of the confinement of the two boundaries in the vertical direction, the quantum behavior of electrons will cause a number of unique properties for thin metal films that could be superior to their bulk counterpart. In particular, quantum size effects on surface reactivity have been studied extensively for applications in catalysis, corrosion, and gas sensing. Here we further consider the dissociation path for O<sub>2</sub> molecules on different Pb(111) films, including both the dissociation along the T- and B- $x, y$  channels from O<sub>2</sub> gases, and the dissociation from molecular adsorption states. After systematic calculations, we find that the most energetically favorable dissociation paths are the same on different Pb(111) films, i.e. from the HH1 adsorption state to the atomic adsorption of two oxygen atoms at two neighboring hollow sites. Figure 9 shows the 2D PES cuts for the O<sub>2</sub> dissociation on 4~7 monolayers Pb(111) films. The calculated energy barriers are respectively 0.26, 0.22, 0.26 and 0.24 eV. Since many properties of Pb(111) films such as work function and surface energy show bilayer oscillation behaviors because of QSE<sup>25</sup>. The even-odd oscillation of the dissociation energy barrier proves the modulation of QSE on the O<sub>2</sub> dissociation on Pb(111) films.

## V. CONCLUSION

In summary, we have investigated the adsorption and dissociation of O<sub>2</sub> molecules on different Pb(111) films. The electronic states of an O<sub>2</sub> molecule in close to the Pb films are firstly analyzed and imply that the adiabatic calculations are reliable. For the molecular adsorption precursor states, we find that the electronic interactions are very similar in the HH1 and HH2 states, and they are thus two nearly degenerate states. Besides, we further point out that no *s-p* hybridizations in Pb(111) films is the main reason for the existence of molecular adsorption precursor states. Based on our adiabatic PES calculations, we find that the dissociation of O<sub>2</sub> from the molecular adsorption precursor states have lower energy barriers than from O<sub>2</sub> gases. The most energetically favorable dissociation paths on different Pb(111) films are found to be the same, which is from the HH1 adsorption state to the atomic adsorption of two oxygen atoms at two neighboring hollow sites. The energy barriers of O<sub>2</sub> on different Pb(111) films are found to be modulated by the QSE of Pb(111) films, and show a bilayer oscillation behavior. Our study further complete the theoretical picture for the adsorption and dissociation of O<sub>2</sub> molecules on different Pb(111) films.

### Acknowledgments

This work was supported by the NSFC under grants No. 10604010, 10904004, and 60776063.

---

\* Corresponding author; zhang\_ping@iapcm.ac.cn (P.Z.).

<sup>1</sup> Busnengo, H. F.; Salin, A.; Dong, W. *J. Chem. Phys.* **2000**, *112*, 7641; Rivière, P.; Salin, A.; Martín, F. *J. Chem. Phys.* **2006**, *124*, 084706.

<sup>2</sup> Kung, H. H. *Transition Metal Oxides, Surface Chemistry and Catalysis*; Elsevier: Amsterdam, 1989; Henrich, V. E.; Cox, P. A. *The Surface Science of Metal Oxides*; Cambridge University Press: Cambridge, 1994.

<sup>3</sup> Błoński, P.; Kiejna, A.; Hafner, J. *Phys. Rev. B* **2008**, *77*, 155424.

<sup>4</sup> Yotsuhashi, S.; Yamada, Y.; Kishi, T.; Diño, W. A.; Nakanishi, H.; Kasai, H. *Phys. Rev. B* **2008**, *77*, 115413.

- <sup>5</sup> Nakatsuji, H.; Nakai, H. *J. Chem. Phys.* **1993**, *98*, 2423.
- <sup>6</sup> Alatalo, M.; Jaatinen, S.; Salo, P.; Laasonen, K. *Phys. Rev. B* **2004**, *70*, 245417.
- <sup>7</sup> Eichler, A.; Mittendorfer, F.; Hafner, J. *Phys. Rev. B* **2000**, *62*, 4744.
- <sup>8</sup> Brune, H.; Wintterlin, J.; Trost, J.; Ertl, G.; Wiechers, J.; Behm, R. J. *J. Chem. Phys.* **1993**, *99*, 2128.
- <sup>9</sup> Österlund, L.; Zorić, I.; Kasemo, B. *Phys. Rev. B* **1997**, *55*, 15452.
- <sup>10</sup> Sasaki, T.; Ohno, T. *Phys. Rev. B* **1999**, *60*, 7824; Honkala, K.; Laasonen, K. *Phys. Rev. Lett.* **2000**, *84*, 705.
- <sup>11</sup> Yourdshahyan, Y.; Razaznejad, B.; Lundqvist, B. I. *Solid State Commun.* **2001**, *117*, 531.
- <sup>12</sup> Yourdshahyan, Y.; Razaznejad, B.; Lundqvist, B. I. *Phys. Rev. B* **2002**, *65*, 075416.
- <sup>13</sup> Kasemo, B. *Phys. Rev. Lett.* **1974**, *32*, 1114.
- <sup>14</sup> Kasemo, B.; Toernqvist, R.; Nørskov, J. K.; Lundqvist, B. I. *Surf. Sci.* **1979**, *89*, 554.
- <sup>15</sup> Katz, G.; Zeiri, Y.; Kosloff, R. *J. Chem. Phys.* **2004**, *120*, 3931.
- <sup>16</sup> Wodtke, A. M.; Tully, J. C.; Auerbach, D. J. *Int. Rev. Phys. Chem.* **2004**, *23*, 513.
- <sup>17</sup> Hellman, A.; Razaznejad, B.; Yourdshahyan, Y.; Ternow, H.; Zorić, I.; Lundqvist, B. I. *Surf. Sci.* **2003**, *532-535*, 126.
- <sup>18</sup> Hellman, A.; Razaznejad, B.; Lundqvist, B. I. *Phys. Rev. B* **2005**, *71*, 205424.
- <sup>19</sup> Zhang, P.; Sun, B.; Yang, Y. *Phys. Rev. B* **2009**, *79*, 165416.
- <sup>20</sup> Lindgren, S.-A.; Wallden, L. *Handbook of Surface Science, Vol.2, Electronic Structure*; Elsevier: New York, 2000.
- <sup>21</sup> Milun, M.; Pervan, P.; Woodruff, D. P. *Rep. Prog. Phys.* **2002**, *65*, 99.
- <sup>22</sup> Zhang, Y.-F.; Jia, J.-F.; Han, T.-Z.; Tang, Z.; Shen, Q.-T.; Guo, Y.; Qiu, Z. Q.; Xue, Q.-K. *Phys. Rev. Lett.* **2005**, *95*, 096802.
- <sup>23</sup> Upton, M. H.; Wei, C. M.; Chou, M. Y.; Miller, T.; Chiang, T.-C. *Phys. Rev. Lett.* **2004**, *93*, 026802.
- <sup>24</sup> Czoschke, P.; Hong, H.; Basile, L.; Chiang, T.-C. *Phys. Rev. B* **2005**, *72*, 075402.
- <sup>25</sup> Wei, C. M.; Chou, M. Y. *Phys. Rev. B* **2002**, *66*, 233408.
- <sup>26</sup> Ma, X. C.; Jiang, P.; Qi, Y.; Jia, J. F.; Yang, Y.; Duan, W. H.; Li, W. X.; Bao, X. H.; Zhang, S. B.; Xue, Q. K. *Proc. Natl. Acad. Sci. USA* **2007**, *104*, 9204.
- <sup>27</sup> Jiang, P.; Wang, L. L.; Ning, Y. X.; Qi, Y.; Ma, X. C.; Jia, J. F.; Xue, Q. K. *Chin. Phys. Lett.* **2009**, *26*, 016803.

- <sup>28</sup> Aballe, L.; Barinov, A.; Locatelli, A.; Heun, S.; Kiskinova, M. *Phys. Rev. Lett.* **2004**, *93*, 196103.
- <sup>29</sup> Yang, Y.; Zhou, G.; Wu, J.; Duan, W. H.; Xue, Q. K.; Gu, B. L.; Jiang, P.; Ma, X. C.; Zhang, S. B. *J. Chem. Phys.* **2008**, *128*, 164705.
- <sup>30</sup> Sun, B.; Zhang, P.; Wang, Z. G.; Duan, S. Q.; Zhao, X. G.; Xue, Q. K. *Phys. Rev. B* **2008**, *78*, 035421.
- <sup>31</sup> Kresse, G.; Furthmuller, J. *Phys. Rev. B* **1996**, *54*, 11169 and references therein.
- <sup>32</sup> Perdew, J. P.; Wang, Y. *Phys. Rev. B* **1992**, *45*, 13244.
- <sup>33</sup> Kresse, G.; Joubert, D. *Phys. Rev. B* **1999**, *59*, 1758.
- <sup>34</sup> Bechstedt, F. *Principles of Surface Physics*; Springer: Verlag Berlin Heidelberg, 2003.
- <sup>35</sup> Weinert, M.; Davenport, J. W. *Phys. Rev. B* **1992**, *45*, 13709.
- <sup>36</sup> Monkhorst, H. J.; Pack, J. D. *Phys. Rev. B* **1976**, *13*, 5188.
- <sup>37</sup> Wyckoff, R. W. G. *Crystal Structures*; Wiley-Interscience: New York, 1965.
- <sup>38</sup> Huber, K. P.; Herzberg, G. *Constants of Diatomic Molecules*; Van Nostrand: New York, 1979.
- <sup>39</sup> Ciacchi, L. C.; Payne, M. C. *Phys. Rev. Lett.* **2004**, *92*, 176104.

## List of captions

**Fig.1** (color online) The electronic density of states for an  $O_2$  molecule in close to the 5 ML Pb(111) film (a), the Mg(0001) surface (b), and the Al(111) surface (c). The Fermi energies are all set to 0.

**Fig.2** (color online) (a) The considered twelve high-symmetry adsorption channels for  $O_2$  on the Pb(111) surface. (b), (c) and (d) The three molecular adsorption states for  $O_2$  at the surface hcp hollow site. Red and grey balls represent O and Pb atoms. There is a Pb atom in the second layer below the HH site to make it distinct from the FH site.

**Fig.3** (color online) (a) Difference charge density for the HH2 adsorption state of  $O_2$  on the 5 ML Pb film. Red and gray atoms represent O and surface Pb. Regions of electrons accumulation/depletion are displayed in blue/yellow, respectively, and the isosurface value is  $\pm 0.02 e/\text{\AA}$ . (b) Contour plots of the difference charge density in the plane that contains the two oxygen atoms and is parallel to the Pb(111) surface.

**Fig.4** (color online) The projected density of states for the 5 ML Pb(111) film (a), Mg(0001) (b) and Al(111) (c) surfaces. The Fermi energies are all set to 0.

**Fig.5** (color online) One-dimensional cuts of the potential energy surfaces and the corresponding O-O bond lengths ( $d_{O-O}$ ) as functions of the  $O_2$  distance  $h$  from the 5 ML Pb(111) film for eight different dissociative channels. The inset in each panel indicates the initial (red circles) and final (green circles) atomic positions of the two oxygen atoms.

**Fig.6** (color online) The projected density of states around the two oxygen atoms at the initial (a), transition (b) and final states (c) along the B- $y$  adsorption channel. The Fermi energies are set to 0.

**Fig.7** (color online) Color-filled contour plots of the potential energy surface for  $O_2$  dissociation on the 5 ML Pb(111) film from HH1 (a) and HH2 (b) states to the atomic adsorption of two oxygen atoms at neighboring hcp and fcc hollow sites, and from HH1 (c)

and HH2 (d) states to the atomic adsorption at two fcc hollow sites, as functions of the O<sub>2</sub> bond length  $d_{\text{O-O}}$  and distance  $h$  (from the surface).

**Fig.8** (color online) The projected density of states around the two oxygen atoms at the initial (a), transition (b) and final states (c) of the dissociation path from the HH1 state to the atomic adsorption of two oxygen atoms at neighboring hcp and fcc hollow sites. The Fermi energies are set to 0.

**Fig.9** (color online) Color-filled contour plots of the potential energy surface for O<sub>2</sub> dissociation on the 4 (a), 5 (b), 6 (c) and 7 ML (d) Pb(111) films from the HH1 state to the atomic adsorption of two oxygen atoms at neighboring hcp and fcc hollow sites, as functions of the O<sub>2</sub> bond length  $d_{\text{O-O}}$  and distance  $h$  (from the surface).

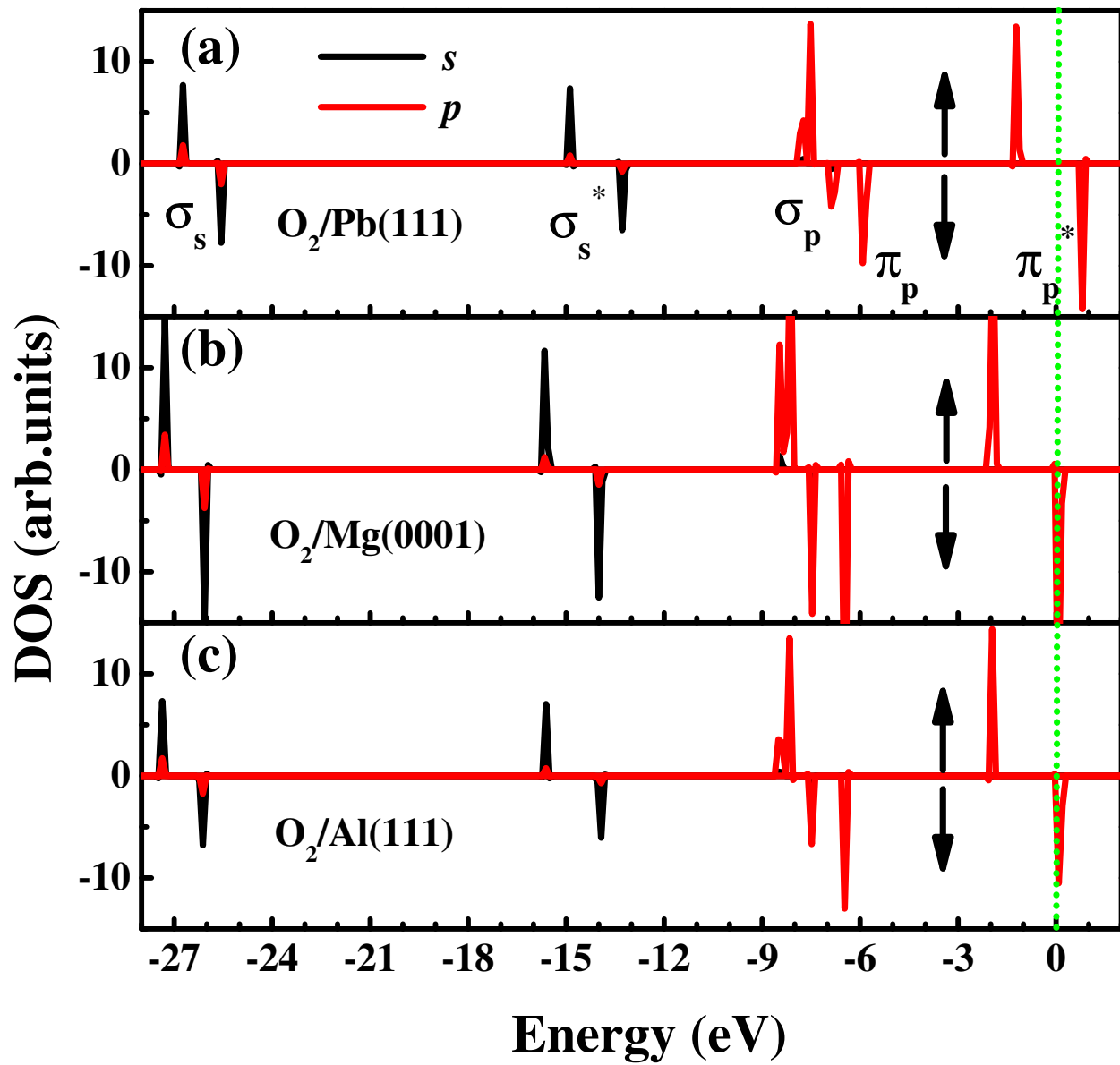


FIG. 1:

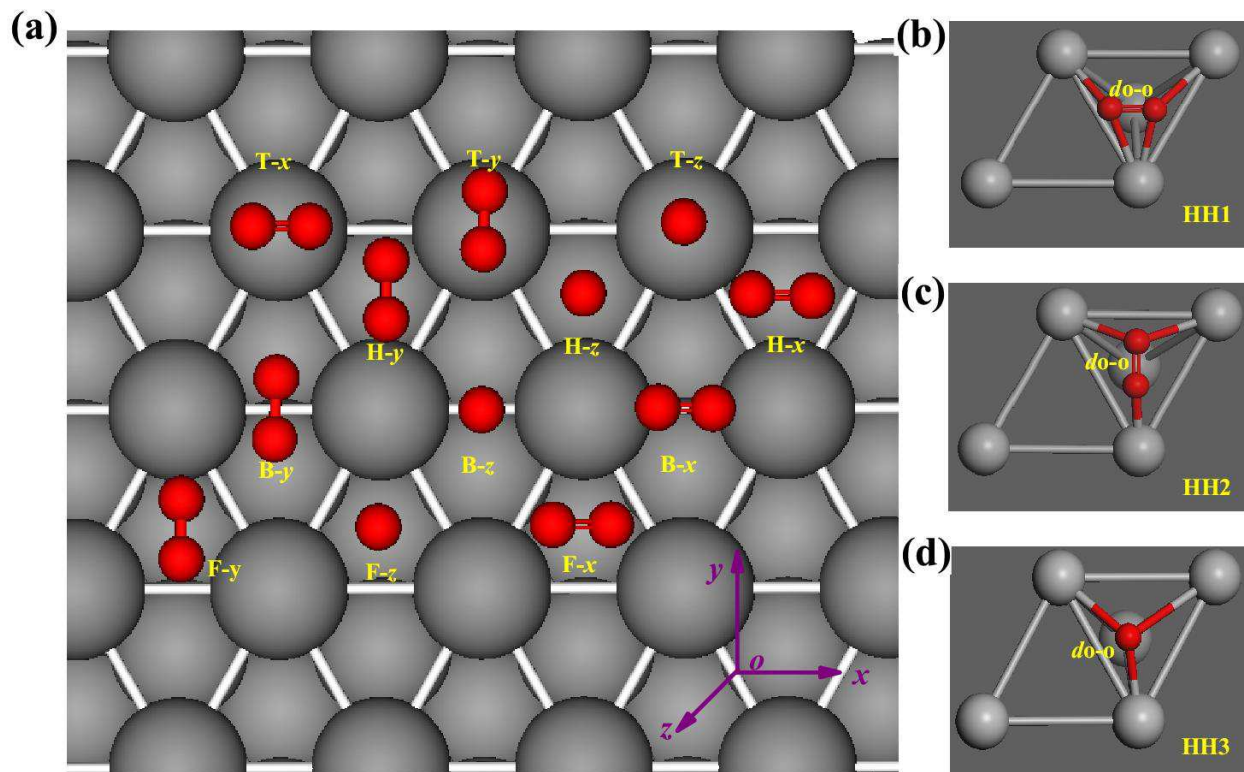


FIG. 2:



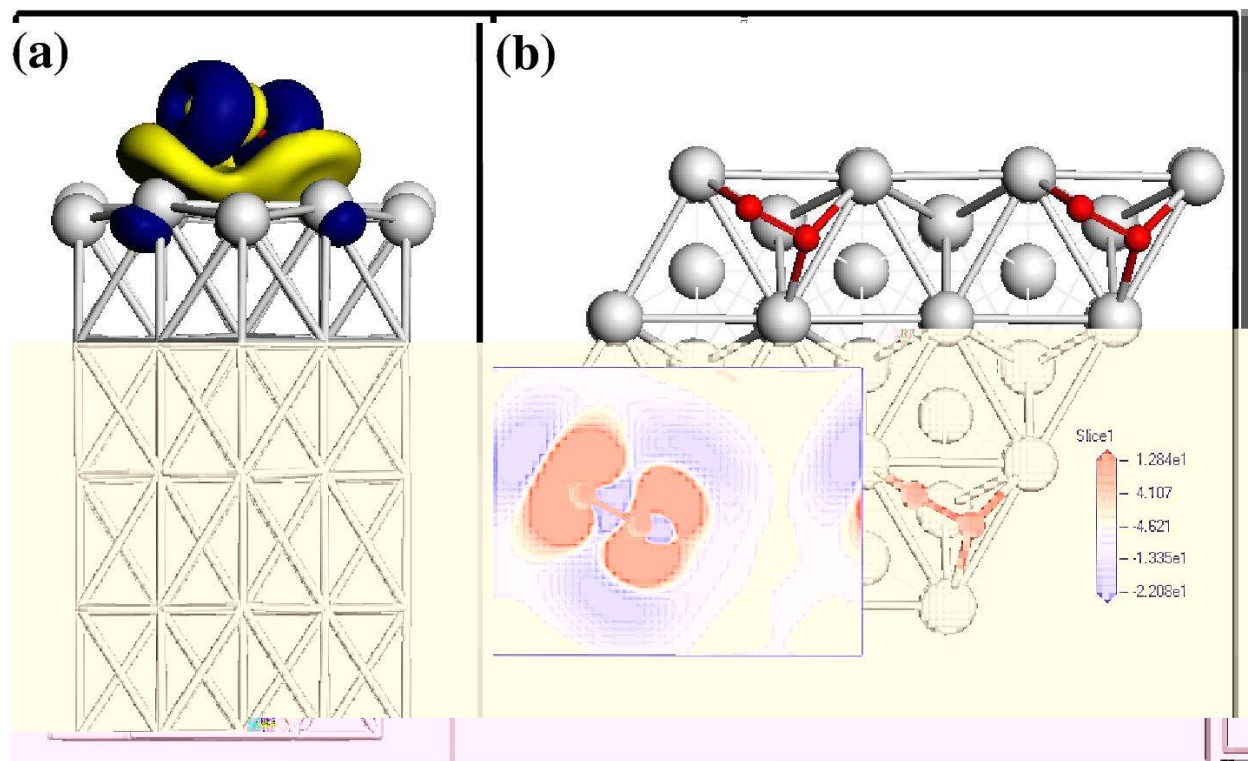


FIG. 3:

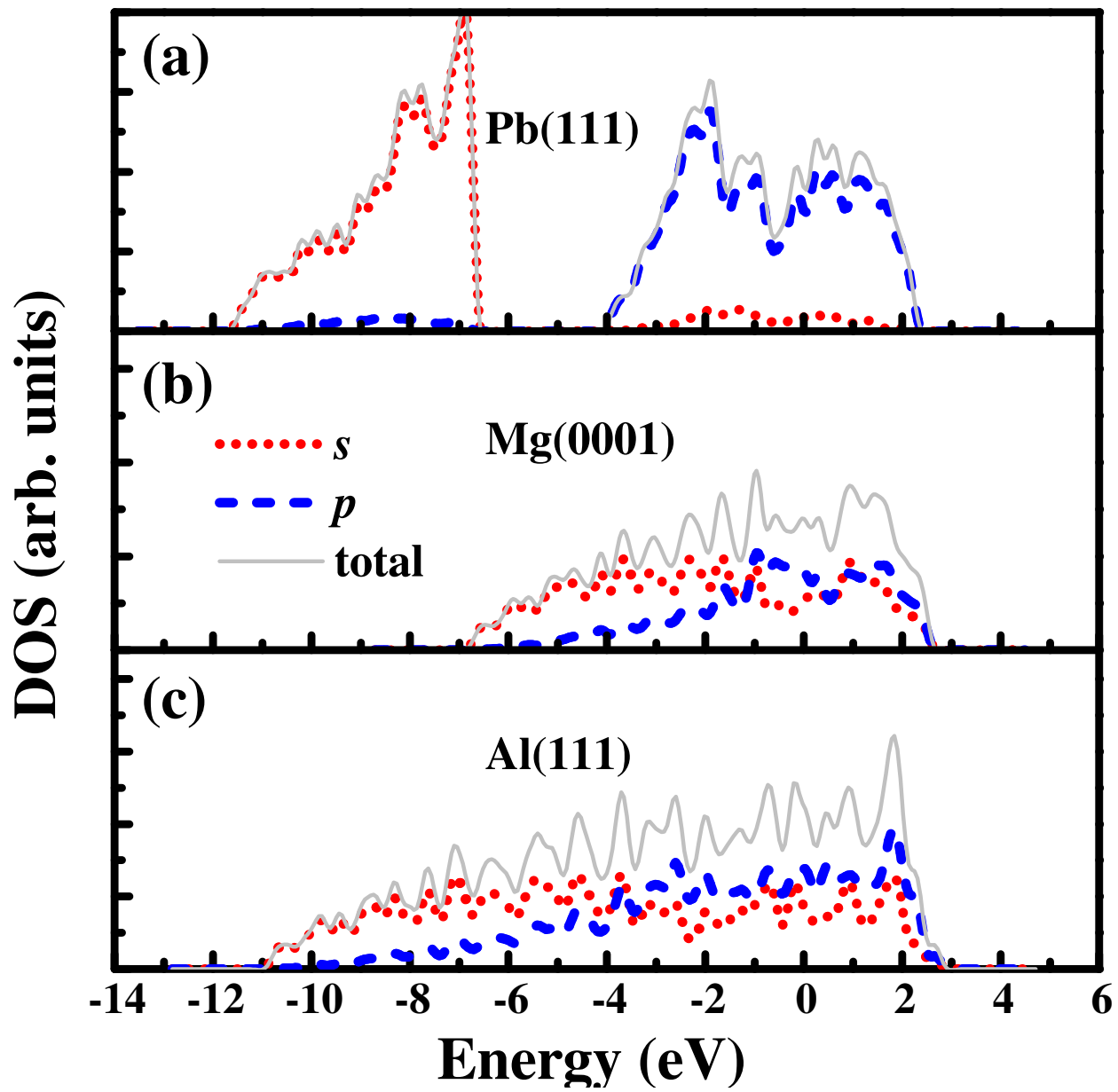


FIG. 4:

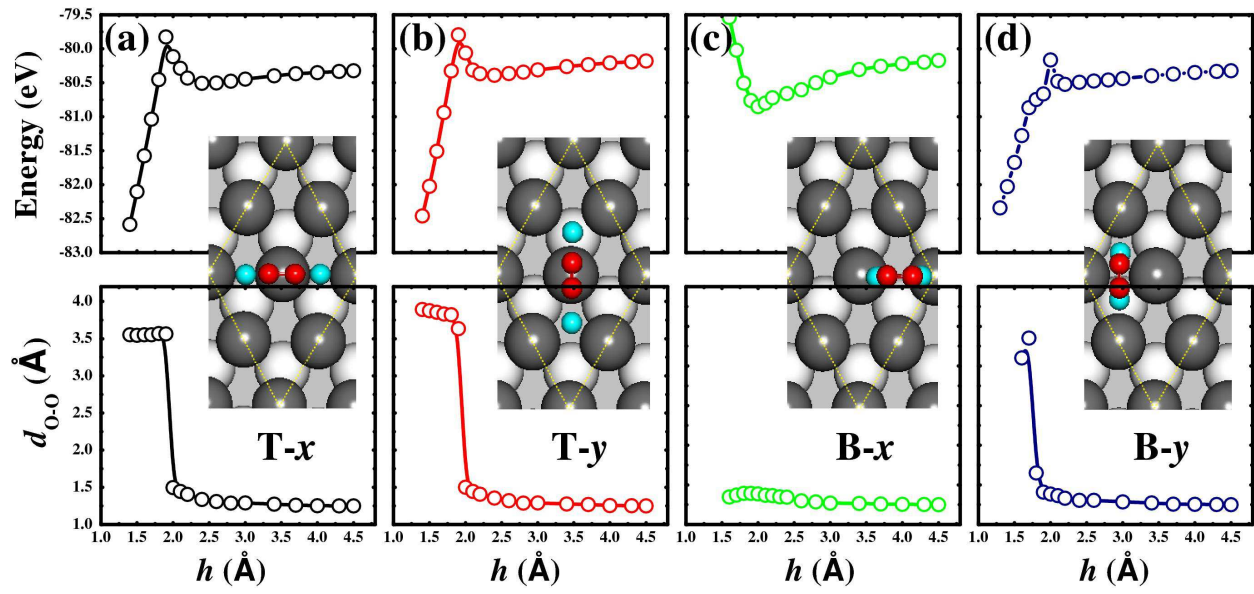


FIG. 5:

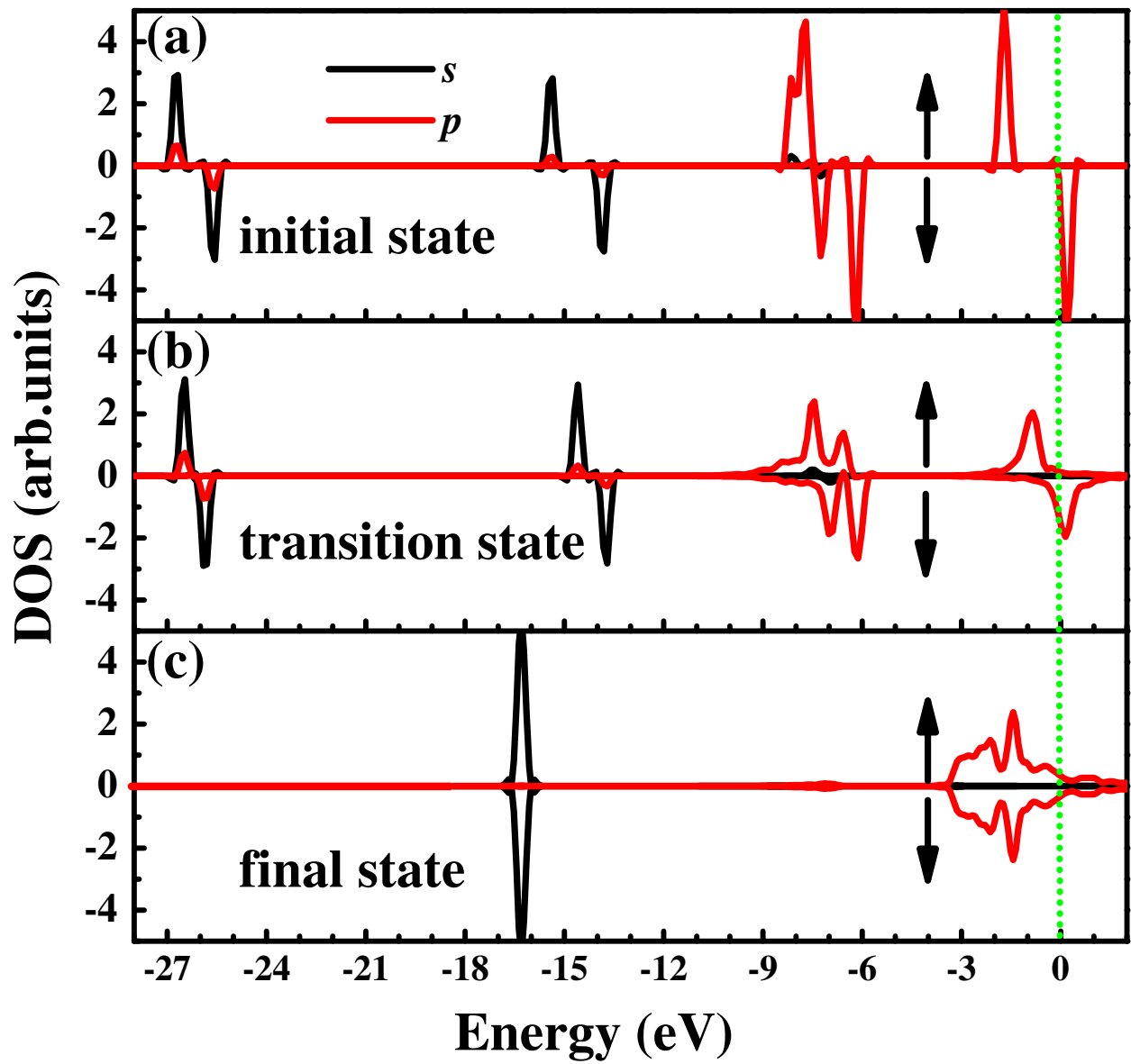


FIG. 6:

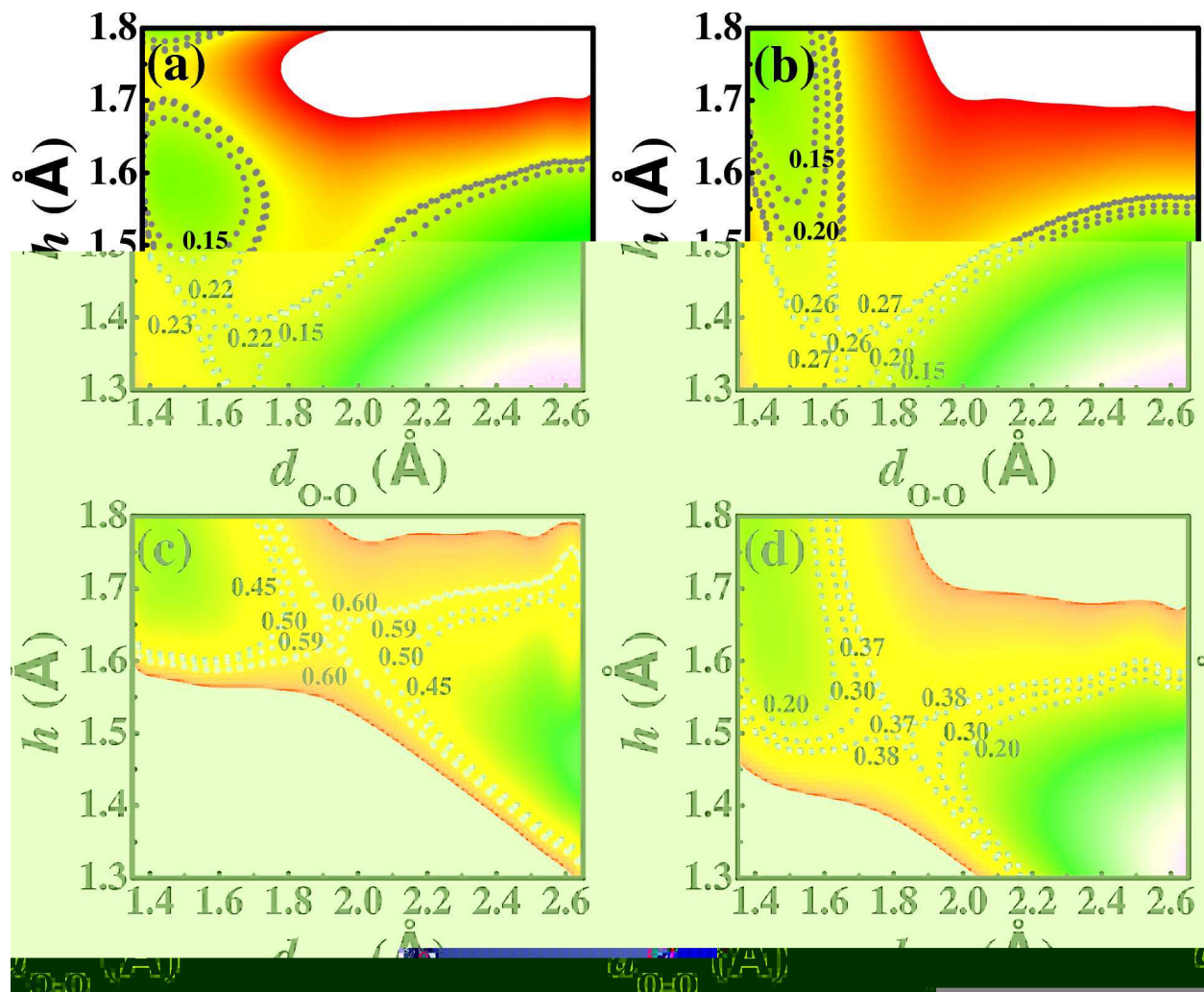


FIG. 7:

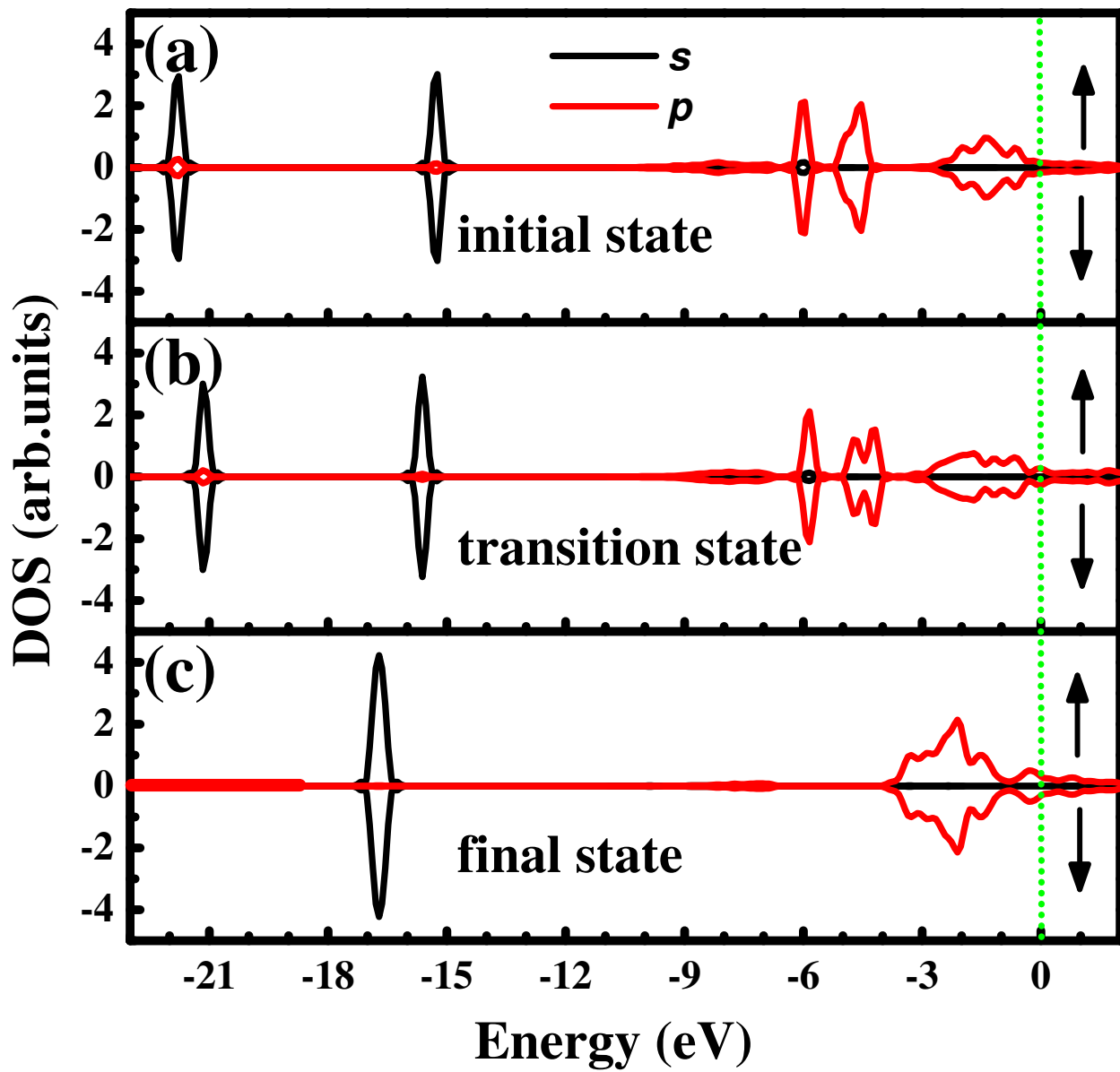


FIG. 8:

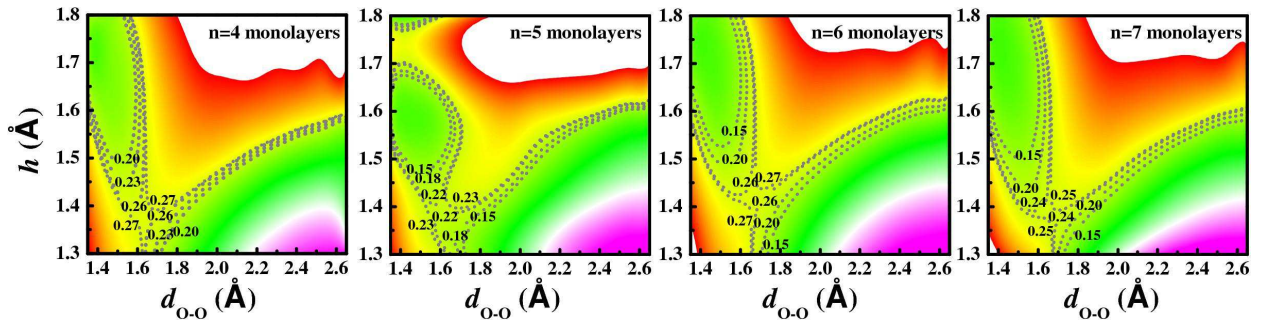


FIG. 9: